Chapter 3

SUDAS: mmWave relaying for 5G outdoor-to-indoor communications

Marco Breiling, Derrick Wing Kwan Ng, Christian Rohde, Frank Burkhardt and Robert Schober

3.1 Introduction

The spatial degrees of freedom offered by multiple antennas at transmitters and receivers of wireless communication systems facilitate a trade-off between multiplexing gains and diversity gains [1–3], which provides a high flexibility in resource allocation. A wireless point-to-point link with M transmit and N receive antennas constitutes an M-by-N multiple-input multiple-output (MIMO) communication system. In particular, under certain mild conditions [1–3], the ergodic capacity of an M-by-N MIMO fading channel increases practically linearly with $\min\{M, N\}$ for a fixed transmit power and bandwidth. Therefore, MIMO has attracted a lot of research interest over the past decades, as it enables significant performance and throughput gains. Unfortunately, the signal processing complexity required in MIMO receivers and the small number of receive antennas that a wireless mobile device can support limit the potential MIMO gain in practice. As an alterative, the concept of cooperative communication has been proposed for wireless networks as an effective technique for realizing the MIMO performance gains. The basic idea of cooperative communication is to enable multiple single-antenna terminals of a multiuser (MU) system to share their antennas to create a virtual MIMO (VMIMO) system [4, 5]. In this context, user cooperation, base station (BS) cooperation, and relaying have been proposed in the literature for implementation of cooperative communications. Theoretically, BS cooperation and user cooperation are able to provide huge performance gains, when compared to non-cooperative networks. However, the required information exchange between BSs via backhaul links [6] and the information exchange between users via wireless channels make these options less attractive in practice. In contrast, cooperative relaying with dedicated relays requires significantly less signaling overhead and allows for low-cost implementations while achieving significant coverage extension, diversity gains, and throughput gains compared to non-cooperative transmission. Therefore, cooperative relaying has attracted significant interest from both academia and industry in the last few years.

In practice, relays can transmit and receive signals at the same time and over the same frequencies, which is known as full-duplex (FD) relaying [7–9]. However,

implementing such FD relays requires precise and expensive hardware components which may not be desirable and cost effective. Alternatively, relays may operate in a half-duplex manner [10–27], i.e., transmission and reception at relays are separated in either time or frequency. Such relays are also known as cheap relays in the literature due to their low hardware complexity. Different relaying strategies such as amplify-and-forward (AF), compress-and-forward (CF), and decode-and-forward (DF) protocols have been proposed in the literature [10–27]. There is no uniformly optimal relaying protocol, and each protocol can outperform the others, depending on the system configuration. Nevertheless, AF is particularly appealing for practical implementation, as the relays only amplify and linearly process the received signal which leads to low-complexity transceiver designs. More importantly, AF relays are transparent to the adaptive modulation techniques that are typically employed at the BSs. For these reasons, AF was selected as one of the possible relaying modes in IEEE 802.16j (mobile multihop relay) and is being proposed for the fourth generation (4G) Long-Term Evolution (LTE) Advanced systems. Despite the significant advances in communication researches in the past decades, the data rate of current 4G systems is still limited, especially for outdoor-to-indoor communication. Besides, it is foreseen that existing network architectures may become a bottleneck in the development of next generation communication. Thus, an effective system architecture to assist outdoor-to-indoor communication is needed.

The remainder of this chapter is organized as follows. In Section 3.2, we provide a brief introduction to next generation communication systems. In particular, we discuss three existing potential technologies for realizing the goals of next generation communication systems. In Section 3.2.3, we propose a novel shared user-equipment side distributed antenna system (SUDAS) to assist outdoor-to-indoor communication which can effectively improve the system data rate. Then, in Section 3.3, practical implementation details of the proposed system are discussed. Sections 3.4 and 3.5 present the mathematical model and numerical performance results for the proposed system, respectively. Finally, in Section 3.6, we discuss some future research and implementation challenges for the designed system.

3.2 5G communication systems

High energy efficiency, low communication latency, high spectral efficiency, and cost effectiveness are the primary goals of the fifth generation (5G) mobile communication systems [28–32]. In particular, a target data rate of 10 Gbit/s per device is expected for both uplink and downlink communications. The data rate originally envisaged for 4G mobile communication standards was 1 Gbit/s, and the LTE-A Release 10 standard extended this target to 3 Gbit/s. The ambitious goal of 5G will enable the download of high-definition (HD) movies within seconds and will offer very high data rates to many users simultaneously. The tenfold increase in the required data rate from 4G to 5G is one of the key performance indicators specified by the European Commission for 5G research within the Horizon 2020 programme. However, with existing technologies, it appears very difficult to reach such high data rates even under favorable conditions. Currently, three technologies are considered as top candidates for realizing

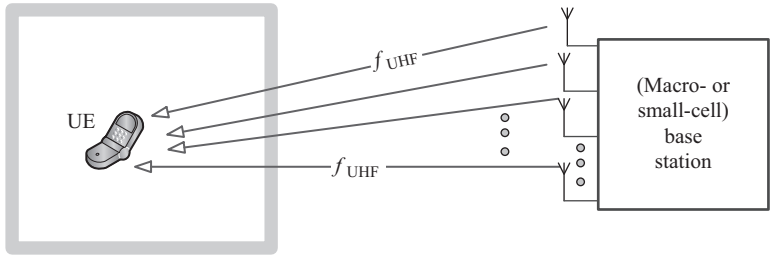

Figure 3.1 A massive MIMO BS serving a UE inside a building in the ultra-high-frequency (UHF) band, f_{UHF}

the 5G goals: massive MIMO, small cells, and the use of unlicensed millimeter wave (mmWave) bands. We will show in the sequel that it is highly questionable whether these technologies alone are able to reach the elusive goal of 10 Gbit/s.

3.2.1 Massive MIMO

In the past decades, MIMO has been implemented in modern communication systems for providing high-speed data rate communication services due to its potential to improve spectral efficiency [1–3]. Especially, massive MIMO technology, where a BS is equipped with a very large number of antennas to serve a comparatively small number of users [33–36], is considered as a potential candidate for achieving the 10 Gbit/s data rate target in 5G, cf. Figure 3.1. However, state-of-the-art smartphones are typically equipped with only two receive antennas which limit the spatial multiplexing gain offered by MIMO. In practice, some expensive user-equipments (UEs) might possess even up to four internal antennas. Yet, deploying more than four receive antennas at each UE may not be realistic due to the limited physical size of mobile receivers. Thus, despite the use of massive MIMO, at most four spatial streams can be exploited simultaneously for increasing the data rate of a UE. On the other hand, with carrier aggregation, a maximum of 200 MHz of licensed spectrum [37] can be created for a single mobile network operator (MNO) with today's technology. In other words, a total of 50 bit/s/Hz spectral efficiency is required to meet the 10 Gbit/s requirement. With a maximum of four spatial streams per UE offered by massive MIMO, 12.5 bit/s/Hz per spatial stream is needed which leads to a minimum required signal-to-noise ratio (SNR) of 38 dB. Besides, the use of at least 16384-quadrature amplitude modulation (QAM) in each stream is needed for achieving the required spectral efficiency. However, the computational complexity for information decoding at the receiver grows exponentially with the size of the constellation, and it is challenging to implement such decoders for real-time applications at a reasonable cost.

3.2.2 Small cells and mmWaves

The concept of small cells, e.g., femtocells, has been proposed as a network architecture for reducing the network power consumption and extending service

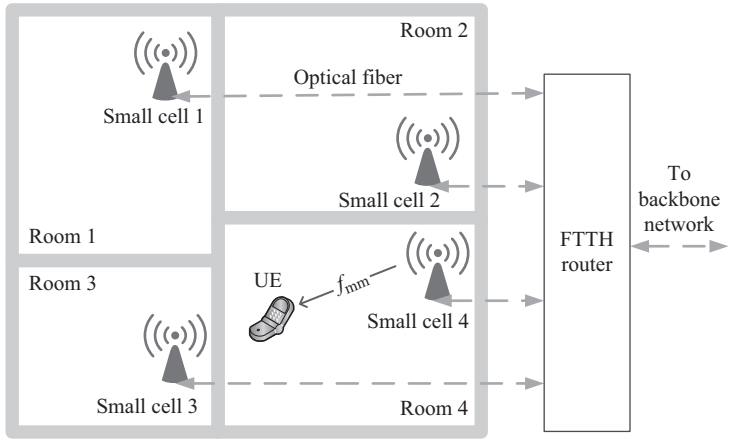

Figure 3.2 An indoor environment equipped with multiple small cells in every room. The small-cell BSs operate in the mmW frequency band, f_{mm}

coverage, cf. Figure 3.2. Thanks to the very large available bandwidth for wireless communication in the mmWave range, e.g., ∼7 GHz of bandwidth in the 60 GHz bands, it appears realistic to deliver 10 Gbit/s from a small-cell BS indoors to a UE over a short distance. However, the bottleneck now becomes the backhauling of the data from a service provider to the indoor small-cell BS. In general, the last mile connection from a backbone network to the terminal users at homes cannot support such high data rates, except if optical fibers are deployed, which is known as fiber-to-the-home (FTTH). However, the cost of deploying FTTH for all home users is prohibitive. For instance, the cost of equipping every building (not home!) with FTTH in Germany is estimated to be around 67 billion € [38]. Moreover, most non-business buildings do not possess an internal optical fiber infrastructure or a wired ethernet for further distribution of the data received from FTTH to the UEs. Furthermore, as mmWave signals are heavily blocked by walls, a small-cell BS transmitting in the mmWave bands would be required in all rooms of a building, cf. Figure 3.2. Hence, extra costs in connecting each room of each building must be added on top of the 67 billion €, and these tremendous costs make this a less attractive option for service providers for realizing the goals of 5G.

Another potential difficulty in utilizing the mmWave bands for communication is finding a suitable location for installing a small-cell BS such that a line-of-sight (LOS) to all UEs is available. Without such a LOS connection, exploiting mmWave links for wireless communication is hardly possible. Observe that if a small-cell BS belongs to a single MNO, the envisaged high data rate is only available to the UEs in the small cell which are associated with this MNO. In order to allow different UEs associated with different MNOs to enjoy high data rate services, the small-cell BS must be neutral with regard to the MNO which is not the case for the small-cell BSs on the market.

3.2.3 Combinations of massive MIMO and mmWave

Recently, different approaches for utilizing a combination of massive MIMO and mmWave have been proposed. Basically, these approaches can be divided into two categories, and we summarize the corresponding disadvantages in the following:

- Backhauling of small cells by massive MIMO over mmWave
  - The problem of this scheme is the high penetration loss of building walls from outdoor to indoor. Specifically, high propagation losses are expected over longer distances at mmWave frequencies.
  - A small-cell BS is required in each room and cannot be shared by different MNOs simultaneously.
- Exploiting massive MIMO for communication to UEs in mmWave band
  - The high penetration loss of walls renders this approach for outdoor use only, i.e., outdoor-to-indoor communication via mmWave may not be supported.
  - A large number of backhauling BSs are needed in order to provide sufficient service coverage for small-cell BSs. Specifically, a LOS connection is required from any UE location to at least one BS at any time.

The combination of massive MIMO and small-cell schemes has limited potential to improve the system performance as long as their operation is limited to the high-frequency unlicensed mmWave bands. Since both licensed and unlicensed bands are available to the service providers, it is reasonable to utilize both spectra to meet the stringent data rate requirements of 5G which motivates our proposed design in the next section. In the last decade, most of the data rate improvement in mobile communication systems was due to the use of MIMO with an increasing number of antennas [4–42]. However, only a small number of UHF antennas can be integrated into a UE which limits the MIMO gain for improving the spectral efficiency. On the other hand, mmWave band communication facilitates small antenna sizes and provides a huge bandwidth for achieving high data rate communication. Yet, mmWave communication suffers from very difficult propagation conditions [43] compared to UHF. Therefore, we propose a system architecture, which efficiently combines the advantages of MIMO over a mobile UHF band channel with its favorable propagation conditions and mmWave with its large bandwidth. Our novel architecture is derived from the idea of VMIMO [4, 39, 40]. It extends the VMIMO concept to the use of mmWave for relaying the MIMO signals transmitted in the UHF band, and to sharing an infrastructure between multiple UEs and multiple MNOs. VMIMO is also known as cooperative MIMO, distributed MIMO, and virtual antenna arrays [4, 39]. A variant of VMIMO, coordinated multi-point (CoMP), has already been implemented in LTE-A at the BS-side, where the received signals are relayed or forwarded to one entity (e.g., a joint signal processing unit) over the backhauling network [40–42].

3.2.4 SUDAS – overview

The ambitious data rate target of 10 Gbit/s for the 5G standard is elusive despite the use of advanced air interface technologies such as massive MIMO, small cells, and mmWave communication links. In order to achieve this high target data rate for UEs

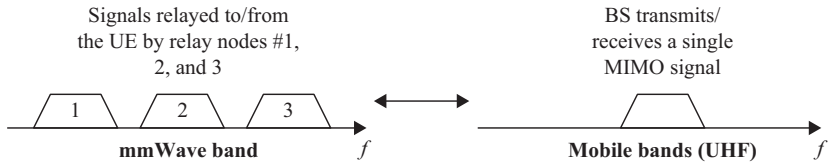

Figure 3.3 Spectrum occupation in the mmWave band and mobile bands (UHF): a single VMIMO carrier in the mobile bands is relayed to multiple non-overlapping signals in the mmWave band

inside a building, we propose in this section for 5G to employ an infrastructure of many low-price relay nodes installed in fixed indoor locations. These nodes relay signals received from the BS in a mobile UHF band via non-overlapping mmWave links to the UE, and vice versa, cf. Figure 3.3. We refer to this scattered infrastructure as a SUDAS [44]. The proposed relaying scheme is limited to only two hops, namely between the BS and the relay nodes, and between the relay nodes and the UE. This simplification allows a low end-to-end latency, and it avoids the significant overhead needed for exchanging routing information. In particular, each relay is called a shared UE-side distributed antenna component (SUDAC) in the proposed SUDAS. In practice, such SUDACs could be integrated into many devices with continuous power supply, including electrical outlets (cf. Figure 3.4), lamps, and light outlets or other devices that carry machine-type-communication (MTC) circuits in the future, such as TV sets and fridges. Besides, the SUDACs are dedicated low-cost devices and scattered in a room. In the following sections, we discuss:

- Working principle of SUDAS
- Potential application scenarios
- Implementation details
- Challenges in SUDAS

3.2.5 SUDAS – working principle

Figure 3.5 illustrates the working principle of the proposed SUDAS. All links in the mobile bands from the BS of MNO "A" utilize the same frequency resource $f_{\mathrm{UHF,A}}$ in the UHF range. Besides, the mmWave links employ the orthogonal frequency bands $f_{\mathrm{mm},i}$, $\forall i \in \{1, \ldots, M\}$, where M is the number of SUDACs. The SUDAS forms a scattered infrastructure which is in contrast to the centralized infrastructure realized by deploying one small-cell BS per room. As shown in Figure 3.5, the SUDAS is not only shared among all UEs in a room but also possibly shared between multiple BSs associated with different MNOs. Because of the high attenuation of stone walls in the mmWave bands, multiple SUDASs located in different rooms do hardly interfere with each other. Therefore, extensive frequency reuse can be deployed in a network with different SUDASs.

The SUDAS concept is particularly promising because it translates spatial multiplexing in the mobile bands (referred to as backend) into frequency multiplexing in the

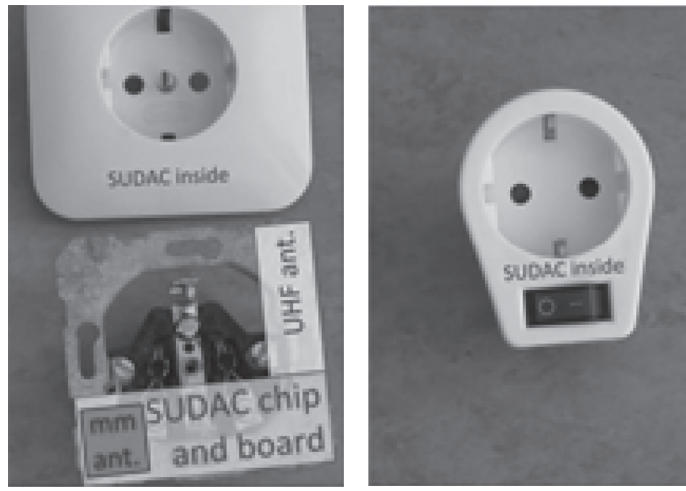

Figure 3.4 Two possible implementations of SUDACs for electrical outlets: (a) integrated into the socket and (b) integrated into an adapter which is to be plugged into a power outlet

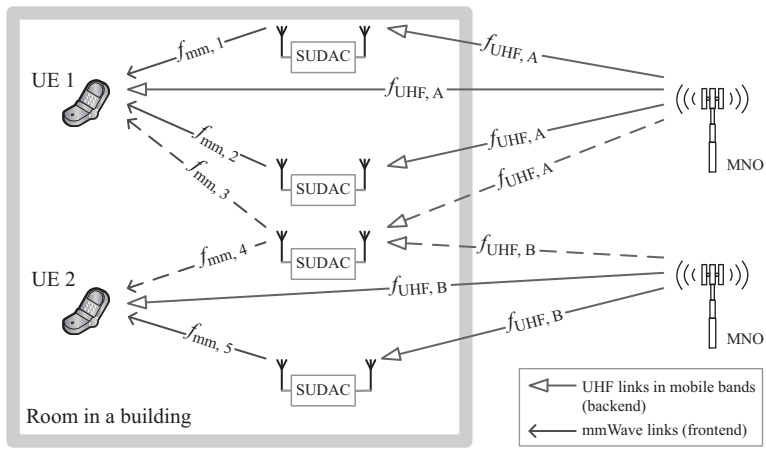

Figure 3.5 Basic principle of a SUDAS for downlink communication. Multiple UEs of different MNOs share the scattered infrastructure represented by the SUDACs via different mmWave frequency bands. Direct links from different MNO BSs to the UEs may exist via different UHF bands

mmWave bands (referred to as frontend), since spatial multiplexing works perfectly in the mobile bands and frequency multiplexing is highly desirable in the mmWave frequency bands. The end-to-end connection between a BS and the UEs is hence split into two segments, and the SUDAS acts as a translator between them. Besides, this

does not preclude the existence of direct links between the BS and the UEs which can be further exploited to improve the VMIMO gain. An advantageous of the SUDACs is that they do not need to carry out information decoding. They simply forward the received signal which will be decoded at the UE (downlink) or the BS (uplink). Similarly, MIMO spatial multiplexing precoding is carried out only at the BS and the UEs, respectively. The SUDACs can hence operate in either an AF or a CF manner. Since signal reception and transmission at each SUDAC have a large frequency separation (one in the UHF band and the other one in the mmWave band), both can take place simultaneously.[1] Different from traditional relaying systems, a SUDAS utilizes both a licensed and an unlicensed frequency band in parallel. As the spectrum in the licensed mobile bands is scarce and costly, its efficient use is a major concern and should be maximized. On the contrary, in the very wide unlicensed mmWave band, high spectral efficiency is not needed as the unlicensed band is virtually free of cost. As a result, SUDAS is able to exploit these properties for improving the system performance. Furthermore, a SUDAS offers markedly higher degrees of spatial diversity than a small-cell BS due to its scattered nature. This is particularly pronounced in the mmWave band. For instance, a human body may completely shadow a mmWave link between a small-cell BS and a UE. However, it is rather unlikely that the links to all SUDACs in a room will be shadowed simultaneously. Also, the SUDAS infrastructure can be shared between multiple UEs and multiple MNOs, which is not possible for traditional relaying networks.

3.2.6 SUDAS – application scenarios

The main application scenario for the utilization of a SUDAS is outdoor-to-indoor communication, i.e., the transmitter is located outdoors while the receivers are inside buildings, such as a living room or a large open-plan office. In fact, since most mobile traffic is consumed indoors (especially at home in the evening [45]) and while commuting, such SUDAS installations would cover the most important mobile use cases. SUDACs could be integrated into electrical outlets and many electrical devices, e.g., Figure 3.4. Therefore, having eight SUDACs or more per room appears to be a realistic scenario. Besides providing very high data rates for one UE, a SUDAS is also able to the improve MU-MIMO performance to support high-speed communication for multiple simultaneous users. In the following, we discuss three different practical application scenarios for which SUDAS is able to improve the system performance.

3.2.6.1 Scenario 1

A SUDAS could enable the data rates and spectral efficiencies that future broadcast systems such as LTE-multimedia broadcast multicast services strive to achieve in order to deliver ultra-HD television content to fixed TV sets (which act as a receive-only UE) with indoor antennas (Figure 3.6). To achieve these goals, the use of MIMO

[1] In practice, the time delay incurred by frequency up-/down-conversion at each SUDAC is much shorter than the delay spread of the channel. Thus, the time delay introduced by the frequency conversion does not have a large impact on the system performance.

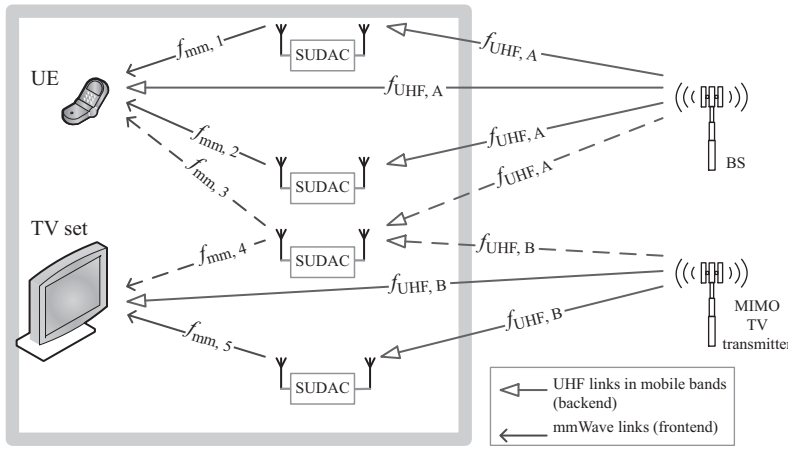

Figure 3.6 A SUDAS used for TV broadcast signal reception with a MIMO TV transmitter and shared by a UE for mobile reception. The TV set can use internal or external indoor antennas

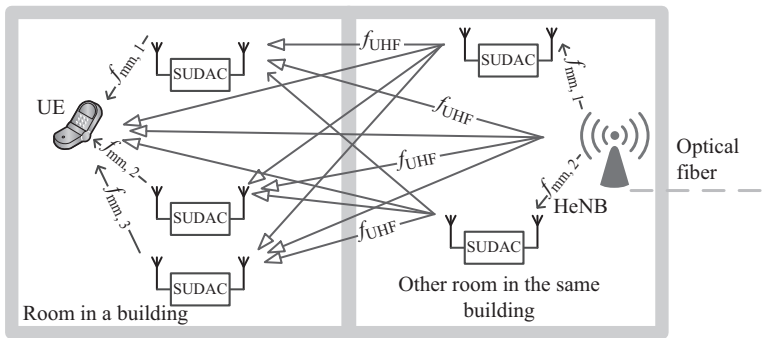

Figure 3.7 SUDAS in two rooms used for connecting a UE to an HeNB in another room

is indispensable and the multiplexing gain brought to the TV set could be increased by the proposed SUDAS.

3.2.6.2 Scenario 2

Figure 3.7 shows another application of the proposed SUDAS. Specifically, a private Home-eNodeB (HeNB) is connected to the public network via optical fiber in one room of the building and can transmit high data rates to UEs in other rooms in the building by first transmitting to the SUDACs in the first room over mmWave. These SUDACs then relay the signal to a sub-6 GHz or UHF band such as the 2.4 GHz industrial, scientific, and medical (ISM) band, where they all transmit concurrently over the same VMIMO channel to another SUDAS in a second room using spatial multiplexing. The second SUDAS finally relays these MIMO signals to the destination

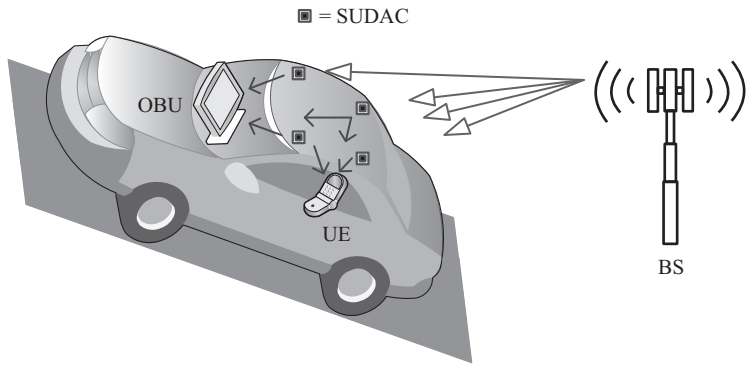

Figure 3.8 BS to vehicle passengers communication via SUDAS

UE once again in the mmWave band. The mmWave transmissions in the first and second rooms do not interfere with each other because of the high attenuation of the walls. In other words, the same mmWave band can be reused extensively. The two new aspects in this scenario are that the HeNB is assisted by several virtual antennas, which can be used in addition to its built-in antennas, and that the UE extends its receiving antennas by the surrounding SUDACs in the same way. The advantage of SUDAS over the existing HeNB concept is hence that rather small devices (HeNB and UE) can share the antennas with SUDACs to achieve higher VMIMO gains.

3.2.6.3 Scenario 3

Besides the installation in indoor devices, another important usage scenario for SUDAS is transportation systems. In particular, SUDACs could be mounted in buses, trains, and cars, too, cf. Figure 3.8. Nowadays, vehicles manufacturers equip cars with multiple antennas to achieve receive diversity for the on-board units (OBU). However, these antennas do not provide data multiplexing gains to the UEs carried by the passengers. As an alternative, the installed antennas could be replaced by SUDACs, and the communication between the antennas/SUDACs and the OBU could thereby be replaced by a standardized wireless air interface operating over mmWave. Then, the UEs of all passengers in the car could benefit from the improved car infrastructure. Possibly, the passengers could employ not only their own car's SUDAS, but even the SUDAS infrastructure of nearby cars could be used when needed, as long as such a resource sharing can be made fair and reasonable. Using an approach similar to the one described above for HeNBs, a device-to-device (D2D) or car-to-car communication between the OBUs of two cars could be established over such a VMIMO link between the two SUDAS, such that higher data rates and/or increased diversity can be achieved.

3.2.7 Comparisons with VMIMO

Existing work on VMIMO covers among others the aspects of channel modeling, analysis of channel capacity and energy efficiency, resource allocation, and routing

algorithms. In some system models, all network nodes have identical functionalities, i.e., any node can be source, destination, and relay, while in other models, there are dedicated source and destination nodes (also dubbed "data-gathering nodes") as well as sheer relaying nodes [10–27]. Moreover, some models are hierarchical and allocate the nodes to groups or layers/stages according to their location or distance to the source node, while simpler models represent a plain uniform network [46]. Most of the systems studied in the literature are partly using in-band relaying, e.g., by using time-division-multiplexing with a first time slot reserved for the hop from a node X to a node Y and a second slot for the hop from Y to Z, or they use short-range links for connecting nearby nodes within one of the aforementioned groups or layers. The model in Reference 4 uses a combination of both, i.e., in-band relaying between the groups and short-range links within a group. Our new proposal uses a simpler system model compared to most of the aforementioned approaches: a SUDAS is a relaying system with only two hops in order to ensure the low latencies required by 5G. As a consequence, routing is not an issue here (it is clear that a SUDAC shall forward the signals to the UE or BS, respectively), and the routing algorithm and associated signaling overhead is omitted. An important property of SUDAS is its use of mmWave for the short-range links to connect each individual "virtual antenna" to a UE. For many devices in a room, a wide spectrum is needed for supporting the links established by the devices. As a result, the mmWave band is perfectly suited for this purpose as the links are almost completely insulated from those in the neighboring rooms. It should be also noted that 5G research already considers D2D links and (multihop) relaying by UEs for other UEs at the cell edge. In contrast to the proposed scheme, 5G does not yet envisage a scattered infrastructure realized by SUDACs that serve not only one mobile network but are shared between multiple MNOs. When relaying is realized by other UEs (as suggested for 5G), then this depends strongly on the goodwill of their owners, who might not be willing to spend their battery energy for relaying the signals of other users. In contrast, since SUDACs are fixed and installed in places with electric power supply (no batteries), these problems do not exist. The infrastructure simply belongs to the owner of the apartment who can make it available to his guests.

3.3 SUDAC – implementation

In practice, a SUDAC can perform AF or CF relaying. In this section, we discuss two different options for the implementation of the out-of-band relaying SUDAC: AF and CF[2].

[2] We note that LTE-A has already enabled both in-band and out-of-band relaying. However, both types of relaying take place in licensed bands. Besides, such relays are (high-cost) regenerative (i.e., DF) relays and represent a centralized infrastructure which is in contrast to the scattered structure of the proposed SUDAS.

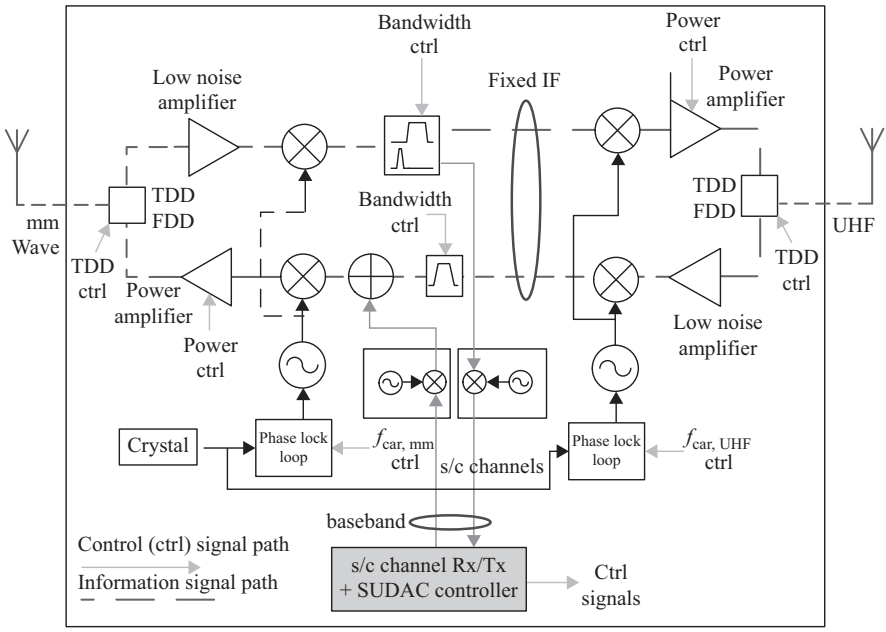

Figure 3.9 A simplified block diagram of an AF SUDAC, where the payload is processed only in the analog domain. Band selection filters in the UHF and mmWave bands have been omitted for specificity

3.3.1 Amplify-and-forward

The main advantage of an AF SUDAC is its potentially low cost and can be implemented with both TDD mode and FDD mode. Figure 3.9 shows a simplified block diagram of such an AF device. The dashed lines denote payload signals which are only processed in the analog domain. In an alternative realization, digital processing can be used, which requires down-conversion of the payload signals to the baseband. The processing (analog or digital) in the SUDAC comprises bandpass filtering in order to avoid the noise amplification and/or relaying of interference surrounding the useful signal. Besides, if the signals can have a flexible bandwidth as required in LTE, then the passband of the bandpass filter has to be dynamically adjusted accordingly. Besides, a SUDAC needs to be configured to know the carrier frequency and bandwidth of the relayed signal. This information can be provided by the UE over a dedicated status/control (s/c) channel in the mmWave band that is frequency-multiplexed with the payload signal.

The s/c channels should carry pilots that enable channel estimation in the mmWave links. Thanks to the high path loss in the mmWave band, the impulse response of an indoor channel is rather short (10–20 ns [47]). This leads to little frequency selectivity over typical bandwidths of up to 20 MHz and simple channel estimation. In the FDD mode, a UE needs to transmit and receive in the mmWave

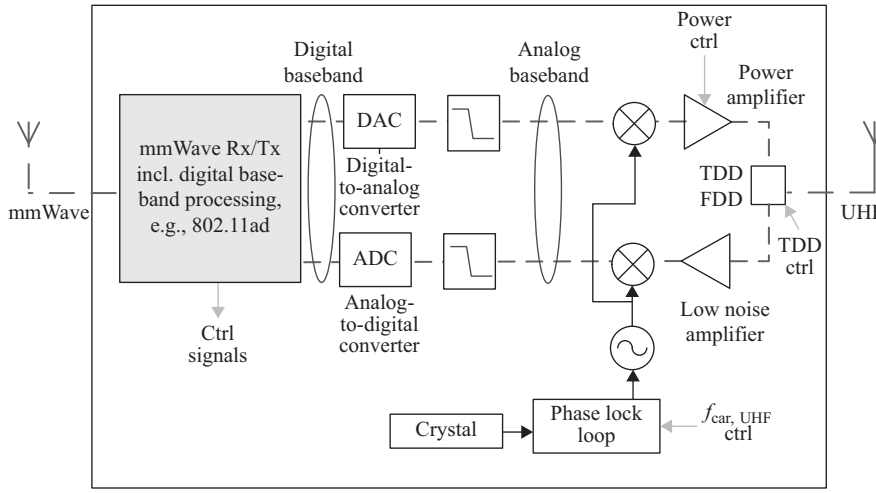

Figure 3.10 Block diagram of a CF SUDAC (either using IEEE 802.11ad or a dedicated air interface). Band selection filters in UHF have been omitted for simplicity

band simultaneously. In order to avoid self-interference due to leakage, the transmit and receive frequency bands have to be separated sufficiently. For applications such as TV reception, unidirectional transmission is used. However, also in this case there needs to be an s/c channel in the return direction to allow handshaking between the UE (i.e., TV set) and the SUDAC for control information exchange. This solitary s/c channel without accompanying payload channel must be sufficiently separated in frequency from the signal in the forward direction to avoid self-interference, of course. Such a solitary s/c channel might also be needed to realize a return link for exchanging control information continuously in the mmWave band, when TDD transmission is used by the BS. Additionally, special rendezvous channels may be needed for the discovery procedure.

Besides the cost, further arguments in favor of an AF SUDAC could be reduced power consumption and a shorter end-to-end latency. However, the price to pay is a lower flexibility than for the solutions presented hereafter. For instance, AF SUDACs are limited to use frequency division multiple access for the mmWave links, while CF SUDACs, as will be discussed in the next section, can employ further multiplexing and multiple access schemes. Moreover, for purely analog AF SUDACs (Figure 3.9), it is difficult to realize fully flexible bandwidths (e.g., from 1.4 to 20 MHz as in LTE) and to equalize the mmWave channel, e.g., compensate the Doppler shift and the slight frequency selectivity. These issues will be discussed later in this chapter.

3.3.2 Compress-and-forward

If the SUDACs are closer to the UEs compared to the BS, the CF protocol provides superior performance compared to AF and DF in relaying networks. Figure 3.10 shows

the block diagram of a CF SUDAC. In the downlink, the signal from the BS received in the mobile (UHF) band is sampled. The corresponding binary representation of the in-phase and quadrature-phase (IQ) samples is then compressed and transmitted over the mmWave bands to the UE. For instance, vector quantization or Wyner-Ziv coding can be applied to CF-SUDAS to compress the observed signal at the SUDAS before sending it to the UEs. In the uplink, the payload from the UE received by the SUDAC contains the binary representation of the IQ samples that are transmitted over the mobile (UHF) band to the BS. This scheme is straightforward, and it is flexible due to the adopted digital baseband signal processing. However, such flexibility comes at the expense of higher cost and/or higher power consumption than other alternative SUDAC realizations.

3.4 Mathematical system model

In this section, we propose a mathematical system model for the AF-SUDAS and evaluate the performance of the proposed SUDAS via simulation.

3.4.1 SUDAS downlink communication model

We consider a mathematical model for a SUDAS assisted orthogonal frequency division multiple access downlink transmission network which consists of one BS, one SUDAS, and one UE, cf. Figure 3.11. The SUDAS consists of M SUDACs, and we assume that the SUDACs are installed in electrical wall outlets and can cooperate with each other by sharing channel state information and received signals via low data rate power line communication links. In other words, joint processing between SUDACs is possible such that the SUDACs can fully utilize their antennas.

The BS is equipped with N_{T} transmit antennas transmitting signals in a licensed frequency band. The UEs are equipped with two set of antennas. The first set consists of R antennas used for receiving signal in the licensed band and the other set consists of one antenna used for receiving signal in the unlicensed frequency band. We focus on a wideband multicarrier communication system with n_{F} subcarriers. The communication channel is time-invariant within a scheduling slot. The BS performs spatial multiplexing in the licensed band. The data symbol vector $\mathbf{d}^{[i]} \in \mathbb{C}^{N_{\mathrm{S}} \times 1}$ on subcarrier $i \in \{1, \ldots, n_F\}$ for the UE is precoded at the BS as

$$\mathbf{x}^{[i]} = \mathbf{P}^{[i]}\mathbf{d}^{[i]}, \tag{3.1}$$

where $\mathbf{P}^{[i]} \in \mathbb{C}^{N_{\mathrm{T}} \times N_{\mathrm{S}}}$ is the precoding matrix adopted by the BS on subcarrier i. The signals received on subcarrier i at the M SUDACs for the UE are given by

$$\mathbf{y}_{\mathrm{S}}^{[i]} = \mathbf{H}_{\mathrm{B}\to\mathrm{S}}^{[i]}\mathbf{x}^{[i]} + \mathbf{z}^{[i]}, \tag{3.2}$$

where $\mathbf{y}_{\mathrm{S}}^{[i]} = [y_{\mathrm{S}_1}^{[i]} \ldots y_{\mathrm{S}_m}^{[i]} \ldots y_{\mathrm{S}_M}^{[i]}]^T$ and $y_{\mathrm{S}_m}^{[i]} \in \{1, \ldots, M\}$ denotes the received signal at SUDAC m. $\mathbf{H}_{\mathrm{B}\to\mathrm{S}}^{[i]}$ is the $M \times N_{\mathrm{T}}$ MIMO channel matrix between the BS and the M SUDACs on subcarrier i and captures the joint effects of path loss, shadowing, and multi-path fading. $\mathbf{z}^{[i]}$ is the additive white Gaussian noise (AWGN) vectors with

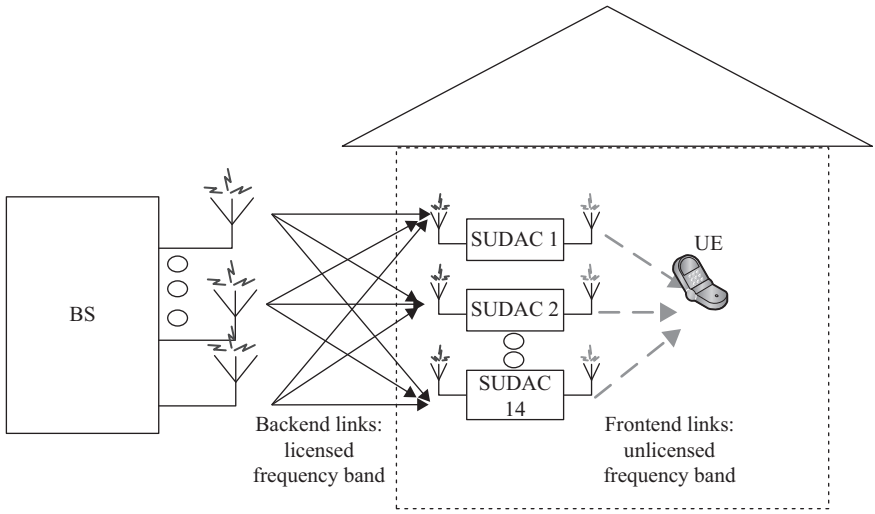

Figure 3.11 SUDAS simulation topology with a BS, $M = 14$ SUDACs, and one UE

distribution $\mathcal{CN}(\mathbf{0}, \mathbf{\Sigma})$ on subcarrier i impairing the M SUDACs where $\mathbf{\Sigma}$ is an $M \times M$ diagonal covariance matrix with each main diagonal element given by N_0.

Then, each SUDAC performs frequency repetition in the unlicensed band. In particular, the M SUDACs multiply the received signal vector on subcarrier i by $\mathbf{F}^{[i]} \in \mathbb{C}^{M \times M}$ and forward the processed signal vector to the UE on subcarrier i in M different independent frequency sub-bands in the unlicensed spectrum, cf. Figure 3.3. In other words, each SUDAC forwards its received signal in a different sub-band and thereby avoids further multiple access interference in the unlicensed spectrum.

Then, the signal received at the UE on subcarrier i from the SUDACs in the M frequency bands, $\mathbf{y}^{[i]}_{\mathrm{S}\to\mathrm{UE}} \in \mathbb{C}^{M\times 1}$, and the BS, $\mathbf{y}^{[i]}_{\mathrm{B}\to\mathrm{UE}} \in \mathbb{C}^{R\times 1}$, can be expressed as

$$\begin{aligned}
\mathbf{y}^{[i]}_{\mathrm{S}\to\mathrm{UE}} &= \mathbf{H}^{[i]}_{\mathrm{S}\to\mathrm{UE}}\mathbf{F}^{[i]}\left(\mathbf{H}^{[i]}_{\mathrm{B}\to\mathrm{S}}\mathbf{x}^{[i]} + \mathbf{z}^{[i]}\right) + \mathbf{n}^{[i]} \\
&= \underbrace{\mathbf{H}^{[i]}_{\mathrm{S}\to\mathrm{UE}}\mathbf{F}^{[i]}\mathbf{H}^{[i]}_{\mathrm{B}\to\mathrm{S}}\mathbf{P}^{[i]}\mathbf{s}^{[i]}}_{\text{desired signal}} + \underbrace{\mathbf{H}^{[i]}_{\mathrm{S}\to\mathrm{UE}}\mathbf{F}^{[i]}\mathbf{z}^{[i]}}_{\text{amplified noise}} + \mathbf{n}^{[i]} \quad \text{and} \\
\mathbf{y}^{[i]}_{\mathrm{B}\to\mathrm{UE}} &= \mathbf{H}^{[i]}_{\mathrm{B}\to\mathrm{UE}}\mathbf{x}^{[i]} + \mathbf{u}^{[i]},
\end{aligned} \tag{3.3}$$

respectively. The m-th element of vector $\mathbf{y}^{[i]}_{\mathrm{S}\to\mathrm{UE}}$ represents the received signal at the UE in the m-th unlicensed frequency sub-band. Besides, since the SUDACs forward the received signals in different frequency bands, $\mathbf{H}^{[i]}_{\mathrm{S}\to\mathrm{UE}}$ is a diagonal matrix with the diagonal elements representing the channel gain between the SUDACs and the UE on subcarrier i in the unlicensed sub-band m. Matrix $\mathbf{H}^{[i]}_{\mathrm{B}\to\mathrm{UE}} \in \mathbb{C}^{R\times N_{\mathrm{T}}}$ is the direct channel between the BS and the UE. $\mathbf{n}^{[i]} \in \mathbb{C}^{M\times 1}$ and $\mathbf{u}^{[i]} \in \mathbb{C}^{R\times 1}$ are the AWGN vector at the UE on subcarrier i in the unlicensed and licensed bands with distribution $\mathcal{CN}(\mathbf{0}, \mathbf{\Sigma})$ and $\mathcal{CN}(\mathbf{0}, \mathbf{\Lambda})$, respectively. $\mathbf{\Sigma}$ and $\mathbf{\Lambda}$ are $M \times M$ and $R \times R$ diagonal

matrices, and each main diagonal element is equal to N_0. In order to simplify the subsequent mathematical expressions and without loss of generality, we assume in the following a normalized noise variance of $N_0 = 1$ at all receive antennas of the SUDACs and the UEs. Besides, $M + R \geq N_S$ and the UE employs a linear receiver for estimating the data vector symbol received in the M different frequency bands in the unlicensed band. The estimated data vector symbols, $\hat{\mathbf{d}}^{[i]} \in \mathbb{C}^{N_S \times 1}$, on subcarrier i are given by:

$$\hat{\mathbf{d}}^{[i]} = (\mathbf{W}^{[i]})^H \begin{bmatrix} \mathbf{y}^{[i]}_{S \to UE} \\ \mathbf{y}^{[i]}_{B \to UE} \end{bmatrix}, \tag{3.4}$$

where $\mathbf{W}^{[i]} \in \mathbb{C}^{(M+R) \times N_S}$ is a post-processing matrix used for subcarrier i at the UE. Without loss of generality, we assume that $\mathcal{E}\{\mathbf{d}^{[i]}(\mathbf{d}^{[i]})^H\} = \mathbf{I}_{N_S}$ where $\mathcal{E}\{\cdot\}$ denotes statistical expectation. As a result, the mean square error matrix for the data transmission on subcarrier i for the UE via the SUDAS and the optimal post-processing matrix are given by

$$\begin{aligned} \mathbf{E}^{[i]} &= \mathcal{E}\{(\hat{\mathbf{d}}^{[i]} - \mathbf{d}^{[i]})(\hat{\mathbf{d}}^{[i]} - \mathbf{d}^{[i]})^H\} \\ &= \left[\mathbf{I}_{N_S} + (\mathbf{\Gamma}^{[i]})^H (\mathbf{\Theta}^{[i]})^{-1} (\mathbf{\Gamma}^{[i]})\right]^{-1} \qquad (3.5) \\ \text{and } \mathbf{W}^{[i]} &= (\mathbf{\Gamma}^{[i]}(\mathbf{\Gamma}^{[i]})^H + \mathbf{\Theta}^{[i]})^{-1} \mathbf{\Gamma}^{[i]}, \qquad (3.6) \end{aligned}$$

respectively, where $\mathbf{\Gamma}^{[i]}$ is the effective MIMO channel matrix between the BS and the UE via the SUDAS on subcarrier i, and $\mathbf{\Theta}^{[i]}$ is the corresponding equivalent noise covariance matrix. These matrices are given by

$$\begin{aligned} \mathbf{\Gamma}^{[i]} &= \mathbf{H}^{[i]}_{S \to UE} \mathbf{F}^{[i]} \mathbf{H}^{[i]}_{B \to S} \mathbf{P}^{[i]} \quad \text{and} \\ \mathbf{\Theta}^{[i]} &= \left(\mathbf{H}^{[i]}_{S \to UE} \mathbf{F}^{[i]}\right) \left(\mathbf{H}^{[i]}_{S \to UE} \mathbf{F}^{[i]}\right)^H + \mathbf{I}_M. \qquad (3.7) \end{aligned}$$

In this following, we first introduce the adopted system performance measure. Then, the resource allocation and scheduling design is formulated as an optimization problem.

3.4.2 System throughput

The end-to-end achievable data rate $R^{[i]}$ on subcarrier i between the BS and UE via the SUDAS is given by

$$R^{[i]} = -\log_2\left(\det\left[\mathbf{E}^{[i]}\right]\right), \tag{3.8}$$

where $\det(\cdot)$ represents the determinant of a matrix. The data rate (bit/s) delivered to the UE can be expressed as

$$\rho = \sum_{i=1}^{n_F} R^{[i]}. \tag{3.9}$$

This system model can be easily extended to a CF SUDAS by following a similar approach as in Reference 48.

Table 3.1 System parameters

Mobile band carrier center frequency	**800 MHz**
mmWave band carrier center frequency	60 GHz
Useful signal bandwidth	200 MHz
Channel model for mobile band to/from BS	Winner+ outdoor-to-indoor
Channel model for mmWave links	IEEE 802.11ad LOS living room scenario
BS antenna height	25 m
Height of SUDAC and UE	1.5 m
Distance BS $\leftrightarrow$ SUDAC	96 m
Distance BS $\leftrightarrow$ UE	100 m
Distance SUDAC $\leftrightarrow$ UE	4 m
Antenna (mobile band) gain of SUDAC and UE	0 dBi
Antenna (mmWave band) gain of SUDAC and UE	3 dBi (semi-isotropic)
Noise figure of SUDAC and UE	8 dB
Maximum transmit power per SUDAC in mmWave	13 dBm

3.5 Numerical results

We focus on a single-cell downlink communication scenario where an LTE-type BS equipped with 16 antennas serves a UE via a SUDAS with 14 SUDACs. The UE is equipped with two mobile band antennas and one mmWave band antenna, while each SUDAC has one mobile band antenna and one mmWave antenna. The important simulation parameters are summarized in Table 3.1. Carrier aggregation is performed such that a total bandwidth of 200 MHz is available in the mobile band for downlink communication. We assume that the downlink channels from the BS to the SUDAS are mutually statistically independent for any pair of BS antennas. Also, in order to reveal the potential of SUDAS, we assume perfect synchronization and channel estimation. Furthermore, we adopt equal power allocation at both the BS and each SUDAC. The system achievable data rate is computed by (3.9).

3.5.1 Average system throughput versus transmit power

Figure 3.12 shows the average system throughput versus the equivalent isotropically radiated power (EIRP) (dBm) for different downlink transmission schemes. As can be seen, both SUDAS with AF and CF relaying realize an extraordinarily high data rate bringing 10 Gbit/s to the indoor UEs over a distance of 100 m. For comparison, we also show the system performance of a benchmark MIMO system and a baseline system. For the benchmark MIMO system, we assume that the UE is equipped with 16 receive antennas without the help of the SUDAS, and optimal resource allocation is performed to maximize the system throughput. In other words, the average system throughput of the benchmark system serves as a performance upper bound for the proposed SUDAS. As for the baseline system, the BS performs optimal resource allocation

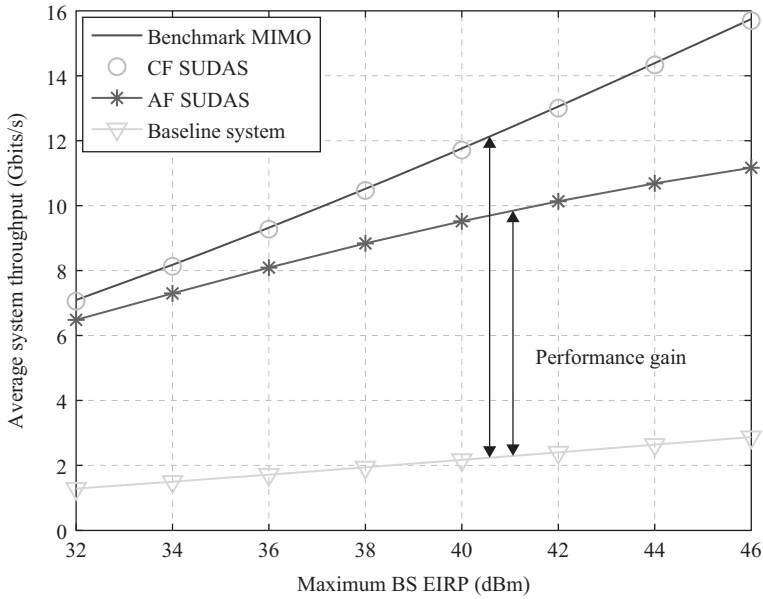

Figure 3.12 Average system throughput (bit/s) versus the EIRP (dBm) for different downlink transmission schemes

and utilizes only the licensed frequency band without the help of the SUDAS and the UE. As can be observed, the proposed SUDAS is able to exploit most of the spatial multiplexing gain, even though the UE is equipped with a small number of receive antennas compared to the BS. Besides, a huge performance gain is achieved by the SUDAS compared to the baseline system as the SUDAS utilizes both the licensed and the unlicensed bands. On the other hand, the performance of the proposed scheme and the benchmark system improves rapidly with increasing BS transmit power budget alleviating the system bottleneck, i.e., the BS-to-SUDAS link.

3.5.2 Average system throughput versus number of SUDACs

Figure 3.13 depicts the average system throughput versus the number of SUDACs for $N_T = 16$. The maximum EIRP of the BS is 46 dBm. It can be observed that the system throughput grows with the number of SUDACs for the proposed SUDAS. In particular, a higher spatial multiplexing gain can be achieved when we increase the number of SUDACs M for $N_T \geq M + 2$. On the other hand, for $M + 2 > N_T$, increasing the number of SUDACs in the system leads to more spatial diversity which also improves the system throughput. Besides, for a large enough number of SUDACs, the performance of the proposed SUDAS closely approaches that of the benchmark system which demonstrates the excellent potential of the proposed scheme in exploiting the spatial multiplexing gain.

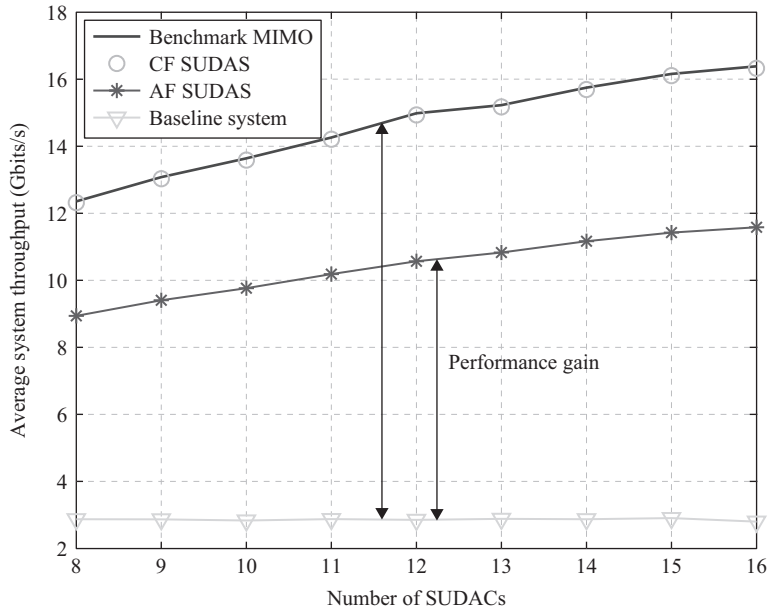

Figure 3.13 Average system throughput (Mbits/s) versus the number of SUDACs for a maximum EIRP at the BS of 46 dBm for different downlink transmission schemes

3.6 SUDAS – challenges

Although the proposed SUDAS has a strong potential to reach the data rate requirements set by 5G, there are many questions and challenges that need to be addressed individually. In this section, we discuss some research challenges arising in the practical implementation of SUDAS for outdoor-to-indoor communication.

3.6.1 Keyhole effect

The SUDAS performance requires suitable channel conditions for creating a VMIMO system from an outdoor BS to an indoor SUDAC. However, it is known that the so-called keyhole effect can lead to performance degradation of the VMIMO channel because of the following three phenomena [49, 50]:

1. Spatial keyholes
2. Diffraction-induced keyholes
3. Modal keyholes

Fortunately, Almers *et al.* [51] show that there is only a negligible spatial keyhole effect if an opening of at least 30 cm × 30 cm exists in a metal wall. As a result, whenever the SUDAS is used in an environment that meets this condition (e.g., rooms with typical window sizes), we can safely assume that spatial keyholes will not affect the

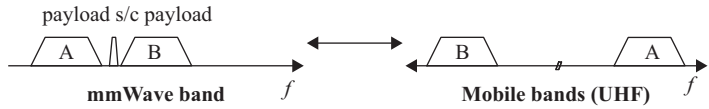

Figure 3.14 Spectrum occupation in mmWave band and mobile bands (UHF): aggregation of multiple mobile carriers in the mmWave band

performance of a SUDAS. On the other hand, Chizhik *et al.* [50] relate diffraction-induced keyholes to outdoor scenarios and also propose a solution for the placement of the BS antennas to counter this effect. Besides, modal keyholes will occur when the waves propagate along hallway-like structures. This could be the case in an indoor scenario or a street canyon. The authors in Reference 49 proposed a relaying system for MIMO which could mitigate such effects. Therefore, it appears that SUDAS will not severely suffer from the above three described keyhole effects. However, further channel measurements and studies should be conducted to verify the channel conditions needed for the successful implementation of SUDAS.

3.6.2 Carrier aggregation

As carrier aggregation will probably be used in 5G, a SUDAS has to allow the relaying of several carriers simultaneously. A simple solution is to assign one SUDAC to one mobile carrier frequency only and to assign further carriers to other SUDACs. Alternatively, several independent RF chains could be bundled in a single SUDAC device. Similarly, several mobile downlink channels could be aggregated inside a SUDAC. For instance, a "double" AF SUDAC could bundle two carriers that are separated in frequency in the mobile bands to adjacent channels in the mmWave band, see Figure 3.14.

3.6.3 Resource allocation for multiple MNOs

As stated before, a SUDAS should allow any UE to connect to the network of their associated MNOs. Thereby, one SUDAS can host different UEs associated with different MNOs concurrently. This must be taken into account by the resource allocation. The resources allocated to a SUDAS are not only the time, frequency, code, and space occupied in the mmWave band but also the relaying (i.e., hardware) resources represented by the pool of SUDACs in the indoor environment. A fair resource allocation must ensure that the available data rates are assigned to each UE according to the quality of service requirements of its services, the number of carriers that can be relayed, and to the UE's and SUDAC's capabilities to support certain carrier frequencies, carrier spacings, bandwidths, channel switching times, transmit powers, etc. Moreover, policies defined by the MNO concerning the data rates granted to certain UEs or services should be taken into account. Besides, the resource allocation must ensure that interference between multiple mmWave links or other users of the mmWave bands (such as IEEE 802.11ad) is avoided.

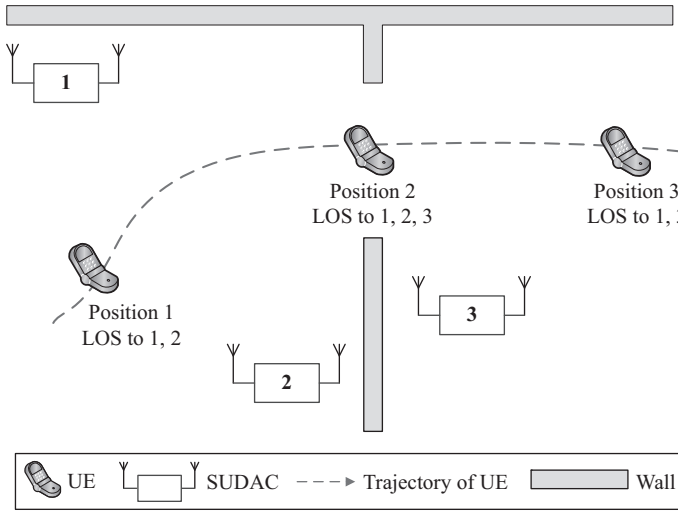

Figure 3.15 New SUDACs discovery scenario

The resource allocation can be implemented in a centralized (e.g., by an entity in the core network cooperating with the other MNOs) or in a distributed manner, cf. e.g., Reference 52. According to our investigations, the best solution appears to be a distributed resource allocation carried out in the UEs but supported by the BSs. The motivation for a distributed resource allocation is among others a lower latency and a lower control plane overhead compared to a centralized approach. In the distributed approach, the UEs can interact with the BSs in order to assist the radio resource management, e.g., in the carrier selection for the mobile bands.

3.6.4 Mobility

Figure 3.15 shows a typical scenario where a UE moves from one room equipped with two SUDACs to another room equipped with one SUDAC. One might wonder whether this system contains two individual infrastructures (one SUDAS per room) or a single larger SUDAS with three SUDACs. The shown trajectory of the UE suggests that that both rooms cannot simply be treated as two separated SUDASs. In position 2, all three SUDACs have a LOS connection to the UE, and the resource allocation algorithm has to cover such cases. Hence, a SUDAS can become a quite extended network of SUDACs, and any UE sees only its local network environment at any time. As the UEs move, the SUDACs must constantly scan passively for approaching UEs and contact them. Then, the resources must be re-allocated locally in the immediate neighborhood of the UE and potentially a hand-over to another SUDAC has to be initiated. Passive scanning should be chosen for the SUDACs in this discovery procedure in order to reduce the electromagnetic pollution and to improve the energy efficiency of the system. With regard to the channel characteristics, the user

mobility causes relatively high Doppler shifts due to the very high carrier frequency in the mmWave band. For instance, moving the UE at 10 km/h when turning around will cause an instantaneous Doppler shift of 550 Hz.

3.6.5 Synchronization and channel estimation

The aforementioned momentary Doppler shift is high but it is still within the range supported by LTE, where the maximum tolerable Doppler frequency is 840 Hz. Therefore, for an AF SUDAC, the UEs or the BS are in principle able to compensate the channel variations over the complete end-to-end link. However, the time-derivative of the Doppler shift can be very high in the mmWave band and might exceed the capabilities of the BS or the UEs. Moreover, indoor SUDACs are fortunately not mobile but installed in a more or less fixed location. Therefore, the channel between the BS and the SUDACs in the mobile bands is frequency selective but quite static, while the channel between the SUDACs and the UEs in the mmWave band is time-variant but affected only by relatively flat fading (over up to 20 MHz bandwidth). Sophisticated AF SUDACs could exploit these properties and compensate the channel variations over the mmWave link, e.g., remove the Doppler shift if required. The situation changes when it comes to the usage of SUDACs in trains, buses, and cars. Now, also the channel between the BS and the SUDAC is time-variant with possibly high Doppler shift. This would add to the Doppler shift originating from the mmWave link, e.g., when the user moves in a train. Hence, the compensation of the Doppler shift by the SUDAC as described above becomes indispensable in the case of AF relaying. On the other hand, for fixed indoor SUDACs installed in an industrial environment such as a factory building, the delay spread may be much longer than the aforementioned 10–20 ns [47]. The longer delays are due to the larger spaces lacking absorbing walls and including metallic reflectors. For such scenarios, the mmWave channel can be quite frequency selective, and an AF SUDAC is unable to compensate these effects. Instead, equalization must be performed at the BS or the UEs. Additionally, the phase noise mask of a mmWave carrier is significantly worse than that typically encountered in mobile UHF bands. An AF SUDAC could compensate part of this phase noise by utilizing the pilots embedded in the s/c channel. Without such compensation, it is questionable whether a BS or a UE would be able to estimate and compensate the phase noise.

3.6.6 Power consumption

With regard to power consumption, according to Reference 53, the total power consumption of a transceiver chip (that processes similar data rates in receive and transmit directions) appears to be governed largely by the power dissipated by the power amplifier. In contrast, the power required for the digital baseband processing (e.g., forward error correction decoding) is probably a minor part compared to the consumption in the power amplifier. As a result, AF and CF SUDASs are expected to consume similar amounts of power, and the choice of the SUDAS relaying protocol may depend more on the hardware complexity.

3.7 Conclusions

In this chapter, we have proposed a novel SUDAS with the objective of achieving the 10 Gbit/s data rate goal set by 5G for indoor UEs. The proposed SUDAS exploits the benefits of the licensed and unlicensed frequency bands simultaneously. In particular, it translates the spatial multiplexing in the licensed bands into frequency multiplexing in the unlicensed bands for boosting the end-to-end data rate via VMIMO. It is expected that the proposed SUDAS can further enhance the system performance when advanced resource allocation technique is employed. Besides, we have also discussed some potential application scenarios where deployment of SUDAS appears to be beneficial. Also, we have investigated different potential realizations of SUDAS and the corresponding implementation challenges. It is expected that the proposed SUDAS is able to bridge the gap between the current technology and the high data rate requirement of the next generation communication systems.

Acknowledgements

This work was supported in part by the AvH Professorship Program of the Alexander von Humboldt Foundation.

References

[1] D. Tse and P. Viswanath, *Fundamentals of Wireless Communication*, 1st ed. Cambridge University Press, United Kingdom, 2005.

[2] A. Goldsmith, *Wireless Communications*. Cambridge University Press, United Kingdom, 2005.

[3] V. K. N. Lau and Y. K. Kwok, *Channel Adaptation Technologies and Cross Layer Design for Wireless Systems with Multiple Antennas – Theory and Applications*, 1st ed. Wiley John Proakis Telecom Series, New York, 2005.

[4] M. Dohler, "Virtual Antenna Arrays," Ph.D. dissertation, Kings College London, University of London, Nov. 2003.

[5] D. W. K. Ng and R. Schober, "Cross-Layer Scheduling Design for Cooperative Wireless Two-Way Relay Networks," *Cooperative Cellular Wireless Networks*, Cambridge University Press, United Kingdom, p. 259, 2011.

[6] D. W. K. Ng, E. S. Lo, and R. Schober, "Energy-Efficient Resource Allocation in Multi-Cell OFDMA Systems with Limited Backhaul Capacity," *IEEE Trans. Wireless Commun.*, vol. 11, pp. 3618–3631, Oct. 2012.

[7] D. Ng and R. Schober, "Dynamic Resource Allocation in OFDMA Systems with Full-Duplex and Hybrid Relaying," in *Proc. IEEE Intern. Commun. Conf.*, Jun. 2011, pp. 1–6.

[8] T. Riihonen, S. Werner, and R. Wichman, "Hybrid Full-Duplex/Half-Duplex Relaying with Transmit Power Adaptation," *IEEE Trans. Wireless Commun.*, vol. 10, pp. 3074–3085, Sep. 2011.

[9] D. W. K. Ng, E. S. Lo, and R. Schober, "Dynamic Resource Allocation in MIMO-OFDMA Systems with Full-Duplex and Hybrid Relaying," *IEEE Trans. Commun.*, vol. 60, pp. 1291–1304, May 2012.

[10] I. Hammerstrom and A. Wittneben, "Power Allocation Schemes for Amplify-and-Forward MIMO-OFDM Relay Links," *IEEE Trans. Wireless Commun.*, vol. 6, pp. 2798–2802, Aug. 2007.

[11] N. Zlatanov, R. Schober, and P. Popovski, "Buffer-Aided Relaying with Adaptive Link Selection," *IEEE J. Select. Areas Commun.*, vol. 31, pp. 1530–1542, Aug. 2013.

[12] N. Zlatanov and R. Schober, "Buffer-Aided Relaying with Adaptive Link Selection-Fixed and Mixed Rate Transmission," *IEEE Trans. Inf. Theory*, vol. 59, pp. 2816–2840, May 2013.

[13] Y. Liu, M. Tao, B. Li, and H. Shen, "Optimization Framework and Graph-Based Approach for Relay-Assisted Bidirectional OFDMA Cellular Networks," *IEEE Trans. Wireless Commun.*, vol. 9, no. 11, pp. 3490–3500, Nov. 2010.

[14] Y. Liu and M. Tao, "Optimal Channel and Relay Assignment in OFDM-Based Multi-Relay Multi-Pair Two-Way Communication Networks," *IEEE Trans. Commun.*, vol. 60, no. 2, pp. 317–321, Feb. 2012.

[15] Y. Liu, J. Mo, and M. Tao, "QoS-Aware Transmission Policies for OFDM Bidirectional Decode-and-Forward Relaying," *IEEE Trans. Wireless Commun.*, vol. 12, pp. 2206–2216, May 2013.

[16] E. Calvo, J. Vidal, and J. R. Fonollosa, "Optimal Resource Allocation in Relay-Assisted Cellular Networks with Partial CSI," *IEEE Trans. Signal Process.*, vol. 57, pp. 2809–2823, Jul. 2009.

[17] Y. Yu and Y. Hua, "Power Allocation for a MIMO Relay System with Multiple-Antenna Users," *IEEE Trans. Signal Process.*, vol. 58, pp. 2823–2835, May 2010.

[18] C. Wang, H. Wang, D. Ng, X. Xia, and C. Liu, "Joint Beamforming and Power Allocation for Secrecy in Peer-to-Peer Relay Networks," *IEEE Trans.* Wireless Commun., vol. 14, no. 6, pp. 3280–3293, June 2015.

[19] C. Li, X. Wang, L. Yang, and W.-P. Zhu, "A Joint Source and Relay Power Allocation Scheme for a Class of MIMO Relay Systems," *IEEE Trans. Signal Process.*, vol. 57, pp. 4852–4860, Dec. 2009.

[20] I. Ahmed, A. Ikhlef, D. Ng, and R. Schober, "Power Allocation for a Hybrid Energy Harvesting Relay System with Imperfect Channel and Energy State Information," in *Proc. IEEE Wireless Commun. Netw. Conf.*, Apr. 2014, pp. 990–995.

[21] Y. Fu, L. Yang, and W.-P. Zhu, "A Nearly Optimal Amplify-and-Forward Relaying Scheme for Two-Hop MIMO Multi-Relay Networks," *IEEE Commun. Lett.*, vol. 14, pp. 229–231, Mar. 2010.

[22] D. Ng and R. Schober, "Resource Allocation for Secure OFDMA Decode-and-Forward Relay Networks," in *12th Canadian Workshop Inf. Theory (CWIT)*, May 2011, pp. 202–205.

[23] D. Ng and R. Schober, "Resource Allocation and Scheduling in Multi-Cell OFDMA Decode-and-Forward Relaying Networks," in *Proc. IEEE Global Telecommun. Conf.*, Dec. 2010, pp. 1–6.

[24] I. Ahmed, A. Ikhlef, D. Ng, and R. Schober, "Optimal Resource Allocation for Energy Harvesting Two-Way Relay Systems with Channel Uncertainty," in *IEEE Global Conf. Signal Inf. Process.*, Dec. 2013, pp. 345–348.

[25] D. Ng and R. Schober, "Cross-Layer Scheduling Design for OFDMA Two-Way Amplify-and-Forward Relay Networks," in *Proc. IEEE Wireless Commun. Netw. Conf.*, Apr. 2010, pp. 1–6.

[26] D. Ng and R. Schober, "Cross-Layer Scheduling for OFDMA Amplify-and-Forward Relay Networks," in *Proc. IEEE Veh. Techn. Conf.*, Sep. 2009, pp. 1–5.

[27] X. Chen, L. Lei, H. Zhang, and C. Yuen, "Large-Scale MIMO Relaying Techniques for Physical Layer Security: AF or DF?" *IEEE Trans. Wireless Commun.*, vol. PP, no. 99, 2015.

[28] J. Zeng and H. Minn, "A Novel OFDMA Ranging Method Exploiting Multiuser Diversity," *IEEE Trans. Commun.*, vol. 58, pp. 945–955, Mar. 2010.

[29] P. Chan and R. Cheng, "Capacity Maximization for Zero-Forcing MIMO-OFDMA Downlink Systems with Multiuser Diversity," *IEEE Trans. Wireless Commun.*, vol. 6, pp. 1880–1889, May 2007.

[30] D. Ng, E. Lo, and R. Schober, "Energy-Efficient Resource Allocation in OFDMA Systems with Hybrid Energy Harvesting Base Station," *IEEE Trans. Wireless Commun.*, vol. 12, pp. 3412–3427, Jul. 2013.

[31] H. Bogucka and A. Conti, "Degrees of Freedom for Energy Savings in Practical Adaptive Wireless Systems," *IEEE Commun. Mag.*, vol. 49, pp. 38–45, Jun. 2011.

[32] A. Chowdhery, W. Yu, and J. M. Cioffi, "Cooperative Wireless Multicell OFDMA Network with Backhaul Capacity Constraints," in *Proc. IEEE Intern. Commun. Conf.*, Jun. 2011, pp. 1–6.

[33] T. Marzetta, "Noncooperative Cellular Wireless with Unlimited Numbers of Base Station Antennas," *IEEE Trans. Wireless Commun.*, vol. 9, pp. 3590–3600, Nov. 2010.

[34] Y. Wu, R. Schober, D. W. K. Ng, C. Xiao, and G. Caire, "Secure Massive MIMO Transmission in the Presence of an Active Eavesdropper," in *Proc. IEEE Intern. Commun. Conf.*, Jun. 2015.

[35] D. W. K. Ng, E. Lo, and R. Schober, "Energy-Efficient Resource Allocation in OFDMA Systems with Large Numbers of Base Station Antennas," *IEEE Trans. Wireless Commun.*, vol. 11, pp. 3292–3304, Sep. 2012.

[36] K. Kumar, G. Caire, and A. Moustakas, "Asymptotic Performance of Linear Receivers in MIMO Fading Channels," *IEEE Trans. Inf. Theory*, vol. 55, pp. 4398–4418, Oct. 2009.

[37] Z. Qi, LTE Throughput Leader Nokia Sets World Record with SK Telecom of Close to 4 Gbps Using TDD-FDD Carrier Aggregation, 2014. [Online] Available: http://nsn.com/news-events/press-room/press-releases/lte-throughput-leader-nokia-sets-world-record-with-sk-telecom-of-close-to-4-gbps-using-tdd

[38] L. D. Heyn, A. Grooten, C. Holden, *et al.*, Cost Model – Country Analysis Report (CAR) for Germany, 2013. [Online] Available: http://www.ftthcouncil.eu/documents/Reports/2013/Cost_Model_CAR_Germany_August2013.pdf

[39] R. Pabst, B. Walke, D. Schultz, *et al.*, "Relay-Based Deployment Concepts for Wireless and Mobile Broadband Radio," *IEEE Commun. Mag.*, vol. 42, pp. 80–89, Sep 2004.

[40] D. Ng, E. Lo, and R. Schober, "Energy-Efficient Resource Allocation in Multi-Cell OFDMA Systems with Limited Backhaul Capacity," in *Proc. IEEE Wireless Commun. Netw. Conf.*, Apr. 2012, pp. 1146–1151.

[41] D. W. K. Ng and R. Schober, "Secure and Green SWIPT in Distributed Antenna Networks with Limited Backhaul Capacity," *IEEE Trans. Wireless Commun.*, vol. 14, no. 9, pp. 5082–5097, Sep. 2015.

[42] D. Ng and R. Schober, "Resource Allocation for Coordinated Multipoint Networks with Wireless Information and Power Transfer," in *Proc. IEEE Global Telecommun. Conf.*, Dec. 2014, pp. 4281–4287.

[43] T. Rappaport, S. Sun, R. Mayzus, *et al.*, "Millimeter Wave Mobile Communications for 5G Cellular: It Will Work!" *IEEE Access*, vol. 1, pp. 335–349, 2013.

[44] M. Breiling, D. W. K. Ng, C. Rohde, F. Burkhardt, and R. Schober, "Resource Allocation for Outdoor-to-Indoor Multicarrier Transmission with Shared UE-Side Distributed Antenna Systems," in *Proc. IEEE Veh. Techn. Conf.*, 2015.

[45] H. Andersson, M. Björn, S. Carson, *et al.*, Ericsson Mobility Report, 2013. [Online] Available: http://ec.europa.eu/digital-agenda/en/news/2014-report-implementation-eu-regulatory-framework-electronic-communications

[46] H. Ding, D. B. da Costa, and J. Ge, "A Centralized Role Selection Scheme for Two-User Amplify-and-Forward Relaying Systems," in *Proc. IEEE Wireless Commun. Netw. Conf.*, Apr. 2013, pp. 3476–3481.

[47] T. Rappaport, J. Murdock, and F. Gutierrez, "State of the Art in 60-GHz Integrated Circuits and Systems for Wireless Communications," *Proc. IEEE*, vol. 99, pp. 1390–1436, Aug. 2011.

[48] J. Jiang, M. Dianati, M. Imran, and Y. Chen, "Energy Efficiency and Optimal Power Allocation in Virtual-MIMO Systems," in *Proc. IEEE Veh. Techn. Conf.*, Sep. 2012, pp. 1–6.

[49] O. Souihli and T. Ohtsuki, "Cooperative Diversity Can Mitigate Keyhole Effects in Wireless MIMO Systems," in *Proc. IEEE Global Telecommun. Conf.*, Nov. 2009, pp. 1–6.

[50] D. Chizhik, G. Foschini, M. Gans, and R. Valenzuela, "Keyholes, Correlations, and Capacities of Multielement Transmit and Receive Antennas," *IEEE Trans. Wireless Commun.*, vol. 1, pp. 361–368, Apr. 2002.

[51] P. Almers, F. Tufvesson, and A. Molisch, "Keyhole Effect in MIMO Wireless Channels: Measurements and Theory," *IEEE Trans. Wireless Commun.*, vol. 5, pp. 3596–3604, Dec. 2006.

[52] R. A. Ramirez, E. Altman, J. S. Thompson, and R. M. Ramos, "A Stable Marriage Framework for Distributed Virtual MIMO Coalition Formation," in *Proc. IEEE Personal, Indoor and Mobile Radio Commun. Symp.*, Sep. 2013, pp. 2707–2712.

[53] A. Jensen, M. Lauridsen, P. Mogensen, T. Sorensen, and P. Jensen, "LTE UE Power Consumption Model: For System Level Energy and Performance Optimization," in *Proc. IEEE Veh. Techn. Conf.*, Sep. 2012, pp. 1–5.